Creating Stable Interfaces in Lithium-Metal Batteries via Initiated Chemical Vapor Deposition Nanoscale Coatings

Ramsay B. Nuwayhid[1], Junghoon Yeom[2], Hunter O. Ford[1], Matthew J. Lefler[1], Rachel E. Carter[3], and Corey T. Love[3]

[1]*National Research Council Postdoctoral Associate, U.S. Naval Research Laboratory, Washington, DC, USA*
[2]*Multifunctional Materials Branch (Code 6354), U.S. Naval Research Laboratory, Washington, DC, USA*
[3]*Surface Chemistry Branch (Code 6170), U.S. Naval Research Laboratory, Washington, DC, USA*

ABSTRACT: Anode-Free Li-metal Batteries (AFLBs) are poised to meet the demands required for high-energy power across a broad range of applications. AFLBs offer substantial improvements in energy density compared to conventional anodes, however are hindered by irreversible Li plating/stripping causing rapid capacity loss and buildup of deleterious solid-electrolyte interphase (SEI) layers. To overcome such hurdles, we employ initiated chemical vapor deposition (iCVD) of polymeric coatings as a means to stabilize the Cu-liquid electrolyte interface and mitigate parasitic reactions giving rise to rapid capacity loss in AFLBs. Nanoscale coatings (7-100 nm) of poly(1,3,5-trivinyl-1,3,5-trimethylcyclotrisiloxane) (pV3D3) are applied to Cu current collectors and characterized vs Li metal in coin-cells. Cycling behavior shows a significant improvement with pV3D3 coatings, resulting in a Columbic efficiency >80% for over 100 cycles, more than double that of uncoated Cu. This is attributed to the moderate Li^+ conductivity of pV3D3 (10^{-7} S/cm) promoting homogeneous Li plating/stripping while minimizing SEI formation. This work provides the mechanistic understanding of iCVD polycyclosiloxane layers on Li plating/stripping and demonstrates the capability of conformal interface engineering for enabling next-generation AFLBs.

Keywords: initiated chemical vapor deposition, Li-metal battery, solid-electrolyte interphase, interface engineering

Introduction

Lithium metal is the ideal anode choice for rechargeable batteries due to its maximum theoretical capacity of 3860 mAh/g and light weight compared to conventional graphite anodes (372 mAh/g). The integration of Li metal into batteries comes with its own set of challenges centered upon the extreme reactivity of the metal, inducing significant precautions required for manufacturing due to the extreme H_2O and O_2 sensitivity of Li. A promising approach to alleviate this issue is the construction of anode-free cells, in which the battery is assembled without an anode material and Li is plated from the cathode onto the negative Cu current collector.[1] Nevertheless, the realization of stable anode-free Li-metal batteries (AFLBs) are hindered by low coulombic efficiency (CE) and the formation of unstable solid-electrolyte interphases (SEI) as a result of heterogeneous Li metal plating and stripping at the Cu current collector.

Thin-film coatings have proved the ability to stabilize reactive interfaces in battery systems through the passivation of electrodes and formation of stable interphases between electrodes-electrolytes.[2, 3] Such coatings are typically ceramic metal oxides deposited by atomic layer deposition (ALD) that inherently require high deposition temperatures (>150 °C) and slow deposition rates (0.1-1 nm/min). Initiated chemical vapor deposition (iCVD) is a similar technique to ALD that has more recently demonstrated an enhanced performance with nanoscale electrode passivation in Li-ion batteries.[4-6] The iCVD technique is attractive for applications in battery systems due to its ability to apply nano-to-micro scale coatings with excellent conformality at ambient temperatures (20-50 °C) and high rates (several nm/min). In this work, nanoscale coatings of poly(1,3,5-trivinyl-1,3,5-trimethylcyclotrisiloxane) (pV3D3) are applied to Cu current collectors to promote homogenous and stable Li metal plating and stripping at the Cu current collector. Through nanoscale (7-100 nm) pV3D3 coatings we observe a significant enhancement in the efficiency of Li metal plating and stripping at the Cu electrode, demonstrating the potential of iCVD coatings to offer improvements in AFLBs. We also characterize the role of the pV3D3 layer on Li plating/stripping mechanistically and offer insights towards iCVD interface optimization.

Results and Discussion

The thickness of pV3D3 thin-films on Cu foils were determined from spectroscopic ellipsometry (SE) measurements on Si wafers that were included with the Cu foil for each batch of pV3D3 deposition. Figure 1a shows the corresponding thickness measurements for deposition times ranging from 5 to 42 minutes. A linear increase in film thickness with time is observed from 5-30 minutes with an average growth rate of 1.4 nm/minute. Above 30 minute deposition times, the growth rate nearly doubles to 2.7 nm/minute. This increase in growth rate is attributed to prolonged substrate heating from the hot filament for the longer depositions. However, despite the increase in growth rate of pV3D3 films with deposition times, a strong agreement is observed for the refractive index of each film shown in Figure 1b. The refractive index curve saturates at 1.52 for the 13 nm pV3D3 film and slightly decreases to a value of 1.50 for 53 nm and 100 nm pV3D3 films. The similar optical properties for pV3D3 films with thickness confirms that the film morphology is consistent from a few nm up to 100 nm.

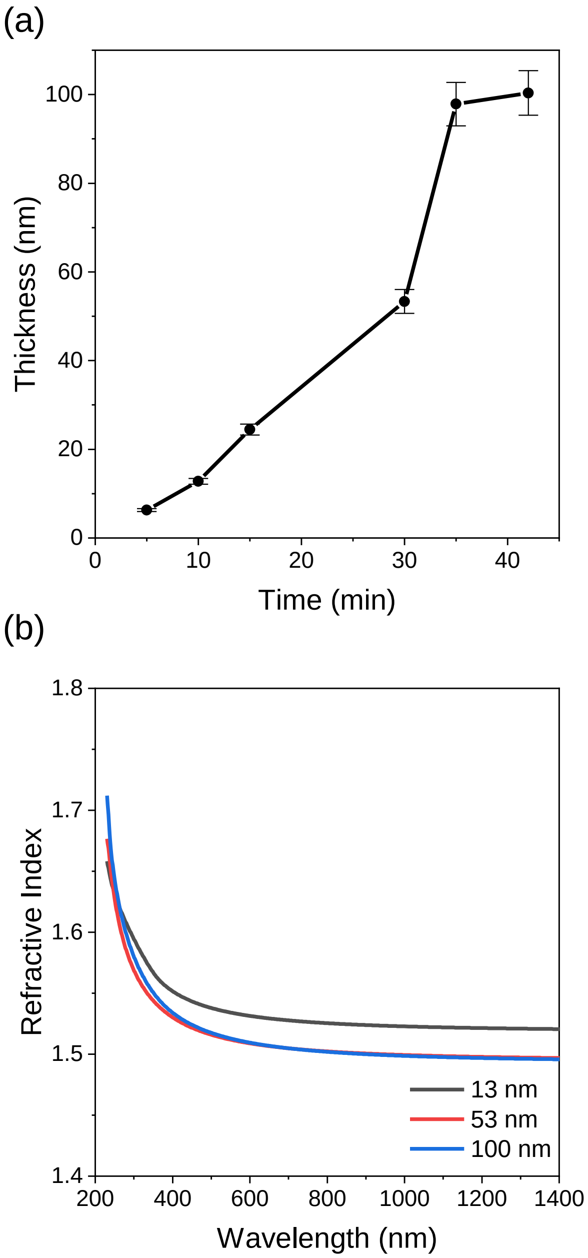

Figure 1. Spectroscopic ellipsometry of pV3D3. (a) Thickness vs. time of pV3D3 depositions. (b) Refractive index as a function of wavelength for 13, 53, and 100 nm pV3D3.

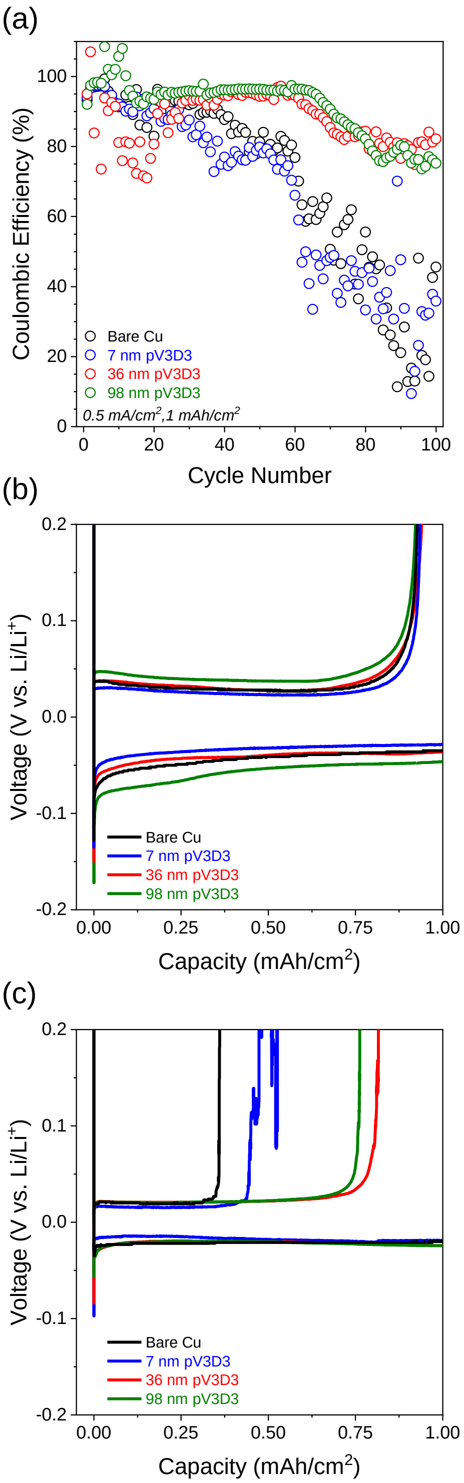

Figure 2. Galvanostatic cycling of bare Cu and pV3D3/Cu electrodes. (a) Coulombic efficiency for 100 cycles. (b) Voltage profiles for cycle 1 and (c) cycle 100. Li metal was plated at a capacity of 1 mAh/cm^2 and charged up to 1 V at 0.5 mA/cm^2 for each cycle.

The effect of pV3D3 on Li metal plating/stripping was evaluated by characterizing the electrochemical cycling efficiency of Li/Cu coin-cells. The cycling performance of bare Cu and pV3D3-coated Cu (7 nm, 36 nm, and 98 nm) cells are summarized in Figure 2. Figure 2a displays the CE of each cell over 100 cycles, in which 36 nm and 97 nm pV3D3 exhibit the highest performance. Both cells retain a CE >90% for ~70 cycles, and slowly decrease to 82% for 36 nm pV3D3 and 75%. The ultrathin 7 nm pV3D3 coating shows minimal improvement to bare Cu, which both electrodes fell below 80% CE after 50 cycles. The individual cycling profiles of each cell are displayed in Figure 2b and 2c for cycle and cycle 100, respectively. The potential for Li nucleation is seen in the large negative voltage spike followed by a plateau region for lithium growth in the discharge curve. The overpotential for Li nucleation in cycle 1 increases linearly with pV3D3 thickness, which is expected for an insulating film in which the dielectric properties become more apparent at higher thicknesses. In Figure 2c, the instability and low capacity of 7 nm pV3D3 is observed displaying heterogeneous voltage spikes during the strip step, whereas 36 nm and 98 nm pV3D3 display stable Li stripping behavior at cycle 100 despite the slight charge capacity drop from cycle 1. These observed phenomena demonstrate the capability of pV3D3 to promote enhanced Li metal plating/stripping.

The surface morphology of electrodeposited Li metal on pV3D3-modified Cu current collectors was characterized with SEM to explain the observed electrochemical phenomena of the Li/Cu cells. Figure 3 shows SEM images of the resulting surface morphology for bare Cu and pV3D3-modified Cu (7 nm and 53 nm). We investigate a 53 nm pV3D3 coating since it is in-between the 36 nm and 98 nm coating thicknesses that resulted in optimum electrochemical performance. In Figure 3a and 3b, bare Cu and 7 nm pV3D3/Cu show similar surface morphologies of Li, in which high surface area Li nucleates are observed in an island-like fashion proceeding towards film growth. This heterogeneous nucleation and growth of Li is known to induces buildup of undesired SEI products leading to the irreversible Li plating/stripping observed in Figure 2.[7] This result implies that the 7 nm pV3D3 has a minimal effect on the interaction of Li with Cu, due to the non-uniform deposition of ultrathin pV3D3 on Cu in such a short deposition time (5 minutes). In Figure 3c, the 53 nm pV3D3 coating is seen to facilitate uniform growth of smooth a smooth Li film, as no exposed areas of the current collector are observed. This supports the evidence for homogeneous and efficient Li plating and stripping for 36 nm and 98 nm pV3D3 coatings observed in Figure 2. The dramatic improvement in surface morphology and electrochemistry with pV3D3 >36 nm is attributed to a uniform and dense pV3D3 passivating the Cu surface, promoting uniform Li$^+$ transport and preventing buildup of SEI on the Li from the liquid electrolyte. Furthermore, the optical images of the 15 mm diameter electrodes in the insets of Figure 3 clearly demonstrate the stark differences in Li interaction with the substrate dependent on pV3D3 coating.

(a) Bare Cu

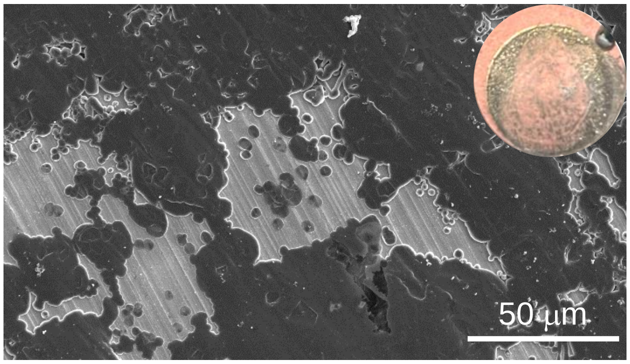

(b) 7 nm pV3D3/Cu

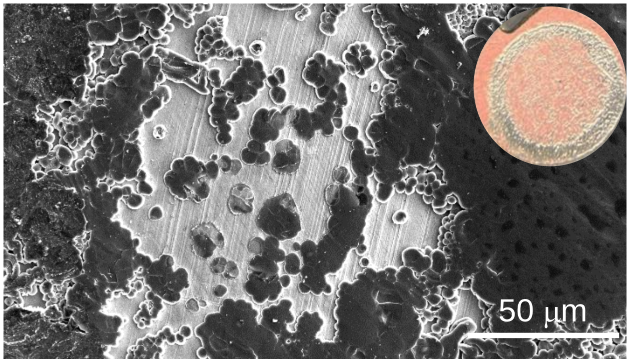

(c) 53 nm pV3D3/Cu

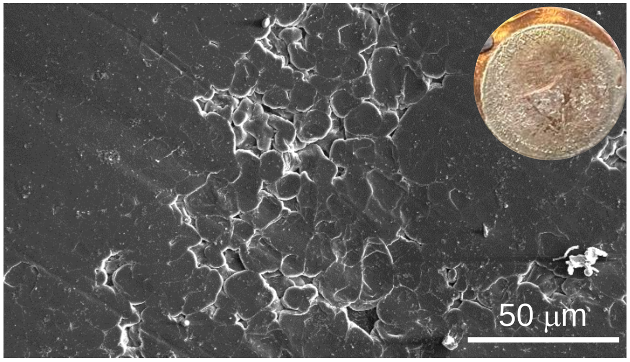

Figure 3. Surface morphology of Li on bare Cu and pV3D3/Cu. SEM image of 1 mAh/cm^2 Li deposit on (a) bare Cu, (b) 7nm pV3D3/Cu, and (c) 53 nm pV3D3/Cu. Optical image shown of each electrode in the inset.

Conclusions

In this work we demonstrate the importance and capability of nanotechnology in improving battery performance. Thin-film iCVD coatings of pV3D3 are observed to have a dramatic effect on the interaction of Li metal with Cu current collectors. Ultrathin coatings (7 nm) display minimal changes than uncoated current collectors, whereas 36-98 nm pV3D3 coatings display a substantial enhancement in coulombic efficiency and Li plating/stripping stability. This enhancement is explained through the uniform film surface morphology of thicker pV3D3 coatings compared to the heterogeneous high surface area Li deposits for ultrathin pV3D3 and bare Cu. This result demonstrates the promising capability of iCVD pV3D3 films to operate as stable interfaces in Li metal and AFLBs.

Experimental Procedures

Cu foils were prepared for iCVD deposition by rinsing with 0.5 M nitric acid, deionized water, and acetone in a stepwise manner, then blown dry with nitrogen. The iCVD depositions were performed in a GVD Corporation reactor. The V3D3 monomer (>95%, Gelest) was heated to 40 °C and the di-tert-butyl peroxide (TBPO 98%, Aldrich) initiator was kept at room temperature. The lines to the reactor were heated to 70 °C and the reactor substrate was held at 25 °C. Depositions were carried out at 200 mTorr with a flow of 1 SCCM TBPO and monomer flow controlled by a ball hand valve. Thermal excitation was achieved by resistively heating a Nichrome filament to 35 V (~2A, 220 °C).

SE characterization was performed on pV3D3 coated Si wafers using a J.A. Woolam M-2000D ellipsometer. Data was collected at variable angles (55° and 75°) and film thickness was modeled using a general oscillator model consisting of Tauc-Lorentz and Gaussian oscillators. The mean-square error for fittings of pV3D3 films <30 nm was 1.8 and increased slightly to 8 for 100 nm films, confirming a high-quality fit of the model to the experimental data.

Half-cells vs. Li metal were assembled in an Ar glovebox for electrochemical testing. A 1M lithium bis(trifluoromethanesulfonyl)imide (LiTFSI) / 0.2M lithium nitrate ($LiNO_3$) in 1,3-diloxolane (DOL) / 1,2-dimethoxyethane (DME) electrolyte was used with Entek gold separators. Charge/discharge measurements were performed on a Maccor cycler, discharging to 1 mAh/cm^2 and charging to 1 V at a rate of 0.5 mA/cm^2.

For SEM characterization, cells were dissembled in an Ar glovebox, rinsed with DME and dried under vacuum, then transferred to the SEM in an air-tight container. A FEI Nova 600 NanoLab SEM was used for imaging at the following conditions: 5.00 kV, 0.80 nA, 5.00 μs dwell time, and 1000x mag.

Acknowledgements

This research was performed while RBN, HOF, and MJL held National Research Council Postdoctoral Associateship Awards at the U.S. Naval Research Laboratory. The authors thank the program officer, Dr. Michele Anderson of the Office of Naval Research, for funding this work under award number N0001420WX01405.

References

1. Nanda, S.; Gupta, A.; Manthiram, A., Anode-Free Full Cells: A Pathway to High-Energy Density Lithium-Metal Batteries. *Advanced Energy Materials* **2021,** *11* (2), 2000804.
2. Zhao, Y.; Zheng, K.; Sun, X., Addressing Interfacial Issues in Liquid-Based and Solid-State Batteries by Atomic and Molecular Layer Deposition. *Joule* **2018,** *2* (12), 2583-2604.
3. Lin, C.-F.; Qi, Y.; Gregorczyk, K.; Lee, S. B.; Rubloff, G. W., Nanoscale Protection Layers To Mitigate Degradation in High-Energy Electrochemical Energy Storage Systems. *Accounts of Chemical Research* **2018,** *51* (1), 97-106.
4. Carter, R.; Parker, J. F.; Sassin, M. B.; Klein, E. J.; Wolak, M. A.; Love, C. T.; Long, J. W., Initiated Chemical Vapor Deposition of Ultrathin Polymer Coatings at Graphite Electrodes for Enhanced Performance in Li-Ion Batteries. *Journal of The Electrochemical Society* **2020,** *167* (6).
5. Reeja-Jayan, B.; Chen, N.; Lau, J.; Kattirtzi, J. A.; Moni, P.; Liu, A.; Miller, I. G.; Kayser, R.; Willard, A. P.; Dunn, B.; Gleason, K. K., A Group of Cyclic Siloxane and Silazane Polymer Films as Nanoscale Electrolytes for Microbattery Architectures. *Macromolecules* **2015,** *48* (15), 5222-5229.
6. Shen, B. H.; Wang, S.; Tenhaeff, W. E., Ultrathin conformal polycyclosiloxane films to improve silicon cycling stability. *Science Advances* **2019,** *5* (7), eaaw4856.
7. Pei, A.; Zheng, G.; Shi, F.; Li, Y.; Cui, Y., Nanoscale Nucleation and Growth of Electrodeposited Lithium Metal. *Nano Letters* **2017,** *17* (2), 1132-1139.